Journal of Cellular Biochemistry 99:647–664 (2006)

# Scribble Associates With Two Polarity Proteins, Lgl2 and Vangl2, Via Distinct Molecular Domains

**Laura M. Kallay,[1,2] Allison McNickle,[1] Patrick J. Brennwald,[3] Ann L. Hubbard,[1] and Lelita T. Braiterman[1]***

[1]Department of Cell Biology, Johns Hopkins University School of Medicine, 725 N. Wolfe Street, Baltimore, Maryland
[2]Department of Physiology, Johns Hopkins University School of Medicine, 725 N. Wolfe Street, Baltimore, Maryland
[3]Department of Cell and Developmental Biology, University of North Carolina, 536 Taylor Hall, Chapel Hill, North Carolina 27599

**Abstract** Scribble (Scrib) is a large multi-domain cytoplasmic protein that was first identified through its requirement for the establishment of epithelial polarity. We tested the hypotheses that Scrib asssociates with the basolateral membrane via multiple domains, binds specific protein partners, and is part of a multimeric complex. We generated a series of EGFP-tagged Scrib fusion proteins and examined their membrane localizations in two types of polarized mammalian epithelial cells using biochemical and morphological approaches. We found that Scrib's Leucine-rich-repeat (LRR) and PDS-95/Discs Large/ZO-1 (PDZ) domains independently associate with the plasma membrane in both cell types. We identified multiple large Scrib complexes, demonstrated that Scrib and the cytoplasmic protein Lethal giant larvae2 (Lgl2) co-IP and that this association occurs via Scrib's LRR domain. Further, this report demonstrates that the membrane protein Vangl2 binds selectively to specific PDZ domains in Scrib. Our identification of Scrib's associations highlights its function in multiple biologic pathways and sets the stage for future identification of more proteins that must interact with Scrib's remaining domains. J. Cell. Biochem. 99: 647–664, 2006. 

**Key words:** Scribble; lethal giant larvae; Vangl2; polarity

This article contains supplementary material, which may be viewed at the Journal of Cellular Biochemistry website at http://www.interscience.wiley.com/jpages/0730-2312/suppmat/index.html.

Abbreviations used: IP, immunoprecipitate; EST, expressed sequence tag; EGFP, enhanced green fluorescent protein; LRR, leucine rich repeat; PDZ, PDS-95/Discs Large/ZO-1; LAP, LRR and PDZ; PBM, PDZ binding motif; WD domain, tryptophan/aspartic acid domain; Mb, membrane; PM, plasma membrane; endo, endogenous; TJ, tight junction; p21 activated kinase; beta-PIX, PAK-interacting exchange factor; Scrib, Scribble; Vangl2, van Gogh-like 2; Dlg1, Discs large 1; Lgl, lethal giant larvae; aPKC, atypical protein kinase C; GUK, guanylate kinase; planar cell polarity; RT, room temperature; BN, blue native; PAGE, polyacrylamide gel electrophoresis; Fr, fraction.

Grant sponsor: NIH RO1; Grant numbers: GM064645, DK63096, DK07632, DK64388; Grant sponsor: Johns Hopkins University School of Medicine.

*Correspondence to: Lelita T. Braiterman, Department of Cell Biology, Johns Hopkins University School of Medicine, 725 N. Wolfe Street, Baltimore, MD 21205.
E-mail: lbraite1@jhmi.edu

Received 7 April 2006; Accepted 18 April 2006
DOI 10.1002/jcb.20992



Scribble (Scrib) is a large cytoplasmic, multi-domain protein that plays many roles in flies, worms, rodent, and humans [Bilder and Perrimon, 2000; Bilder et al., 2000; Nakagawa and Huibregtse, 2000; Murdoch et al., 2003; Nakagawa et al., 2004; Segbert et al., 2004]. Genetic studies in *D. melanogaster* have demonstrated Scrib's importance in the establishment of apical-basal polarity and as a tumor suppressor [Bilder et al., 2000]. Furthermore, its expression is required in flies for the proper basolateral membrane localization of lethal giant larvae (Lgl), another tumor suppressor and cell polarity protein. In mouse, a point mutation in Scrib causes severe defects in neural tube development as do mutations in the membrane protein Vangl2 (also called Ltap or Lpp1) [Montcouquiol et al., 2003; Murdoch et al., 2003], which interacts genetically with Scrib [Murdoch et al., 2001].

Biochemical studies of Scrib in mammalian cells point to a potential link between its roles in polarity and tumor suppression, since its downregulation by the high risk human papilloma-virus E6 protein is correlated with loss of apical-basal polarity [Nakagawa and Huibregtse, 2000] and neoplasia [Nakagawa et al., 2004]. Scrib is also involved in regulated exocytosis through its association with beta-PIX, a guanine nucleotide exchange factor [Audebert et al., 2004].

Scrib is a member of the LAP (LRR (leucine rich repeats) and PDZ (PSD-95/Discs Large/ZO-1)) protein family [Bryant and Huwe, 2000; Santoni et al., 2002]. LRR domains are composed of short motifs of 23 amino acids (aa), which can be repeated 2–23 times to form a broad range of structures [Kobe and Kajava, 2001; Kajava and Kobe, 2002]. Scrib has 16 LRRs at its N-terminus, followed by a LAP-specific domain, a linker region, four non-identical PDZ domains and a substantial C-terminus lacking any identifiable motifs [Santoni et al., 2002]. PDZ domains, composed of 80–100 residues, organize multi-protein complexes by binding short peptide sequences generally found at the extreme C-terminus of transmembrane proteins [Harris and Lim, 2001; Hung and Sheng, 2002].

Given the multiple domains in Scrib and its basolateral localization, we hypothesized that it associates with the membrane via multiple domains and interacts with several partners which genetic studies in flies have predicted [Bilder and Perrimon, 2000; Bilder et al., 2000]. To test our hypothesis, we generated a series of EGFP-tagged Scrib fusion proteins and examined their membrane localizations in two types of polarized mammalian epithelial cells. We found that the LRR and PDZ domains independently associate with the PM in both cell types. Although there are numerous reports identifying Scribble binding proteins, none have found that Scrib binds the cytoplasmic protein Lgl. We used velocity gradients to separate protein complexes then SDS–PAGE and blue native (BN)–PAGE analysis to characterize possible Scrib/Lethal giant larvae2 (Lgl2) associations. Importantly, we found multiple Scrib complexes, documented a Scrib/Lgl2 association and demonstrated that the Lgl2 bound to Scrib via the latter's LRR domain. Finally, we demonstrated that the membrane protein Vangl2 bound selectively to specific PDZ domains in Scrib.

## MATERIALS AND METHODS

### Materials

Defective adenovirus DNA, Psi5ΔE1-E3, pAdLox, and CRE8 cells were provided by S. Hardy [Hardy, 1997] and the pAdShuttle was provided by B. Vogelstein [He et al., 1998]. Reagents and suppliers were as follows: HEK293A cells (QBI293 cells, Qbiogene, Carlsbad, CA); Effectene, QIAprep Spin Miniprep Kit, and Qiagen plasmid Maxi Kit (QIAGEN, Inc., Valencia, CA); Supersignal West Pico Reagent and Sulfolink coupling gel (PierceBiotechnology, Rockford, IL); EGFP-C3 (Clontech, Palo Alto, CA); pGEM T-Easy vector (Promega, Madison, WI); AdEasy competent bacteria (Stratagene, La Jolla, CA); pcDNA3.1-V5-His TOPO vector and Lgl2 IMAGE EST clone: 1886537 (Invitrogen Corp, Carlsbad, CA); Protein A agarose (Sigma, St. Louis, MO). Scribble and Vangl2 EST clones, HA01022 and HA01022S1, and KIAA1215, respectively, were obtained from KAZUSA DNA Research Institute, Chiba, Japan. hLgl1 and hLGL2 EST clones, IMAGE: 2307829 and 5575350, respectively, were obtained from ATCC (Manassas, VA). Other molecular biology reagents were from New England Biolabs (Beverly, MA), Invitrogen Corp, or Promega. Primer synthesis, peptide synthesis, and DNA sequencing were performed at the DNA Synthesis and Sequencing Facility, Johns Hopkins University. Primer synthesis was also performed by Integrated DNA Technologies, Inc., Coralville, IA.

Primary antibodies were from the following sources: goat anti-Scribble (C-20 sc-11049, Santa Cruz, CA); rabbit and mouse anti-GFP (A-6455 and A-11120, respectively) and Alexa-labeled secondary antibodies (Molecular Probes, Eugene, OR); mouse monoclonal anti-α-tubulin, clone DM1A (T9026, Sigma); mouse anti-E-cadherin (610182, Transduction Labs, Lexington, KY); mouse anti-V5 (46-0705, Invitrogen Corp, and MCA1360, Serotec, Raleigh, NC); mouse anti-SAP97/Dlg (VAM-PS005, Stressgen, Victoria, BC, Canada). Rabbit anti-aminopeptidase N (APN) was described previously [Barr and Hubbard, 1993] and rat monoclonal anti-ZO-1 hybridoma cells (R40.76) were provided by B. Stevenson (University of Alberta, Edmonton, Canada). Horseradish peroxidase-conjugated secondary antibodies (donkey anti-rabbit, rabbit anti-goat, and goat anti-mouse), Random Primed DNA Labeling Kit and

$^{32}$P-dCTP-α, were from Amersham Pharmacia Biotech (Piscataway, NJ).

Antisera to Lgl2 was generated in rabbits immunized with a GST-fusion containing the C-terminal 153 residues of Lgl2. Antisera was affinity purified as described previously for Lgl1 [Musch et al., 2002] except that the antisera was cross-absorbed against GST-Lgl1 C-terminus prior to the final affinity purification. This pre-adsorption step was also included in purification of the Lgl1 antibodies used in Figure S1.

### Molecular Biology Techniques

The EGFP-Scrib fusion protein constructs are listed in Figures 2 and 3. EGFP-95–1630 (pYC42) was generated by ligating the *Eco*RV/*Spe*I fragment from clone HA01022 into *Sma*I/*Xba*I digested EGFPC2 vector (Clontech), then its *Age*I/*Mfe*I fragment was ligated to *Xma*I/*Eco*RI digested pAdlox (#6, pLK01). EGFP-N-terminal Scrib and PDZ domain constructs were generated by amplification of HA01022S1 with the following primer pairs: nAH138/nAH192 (#2 N-half, aa1-728); nAH138/nAH111 (#3 EGFP- to AR, aa1-649); nAH138/nAH142 (#4 EGFP-LRR/LAP, aa1-420); nAH138/nAH207 (#5 EGFP-LRR, aa1-381); nAH62/nAH63 (#9 EGFP-C-half, aa727-1630); nAH62/nAH90 (#10 EGFP-PDZ 1-4, aa727-1202); nAH91/nAH63 (#11 EGFP-C-term, aa1197-1630); nAH 180/nAH181 (EGFP-PDZ 1-2, aa720-960); nAH214/nAH215 (EGFP-PDZ 2-3, aa816-1114); and nAH182/nAH183 (EGFP-PDZ 3–4, aa961-1202). All 5′ primers encoded a *Hin*dIII site and 3′ primers nAH142, nAH181, nAH183, nAH192, and nAH 215 encoded a stop codon followed by a *Mfe*I site to facilitate in-frame cloning. PCR products were cloned into pGEM-Teasy and sequences were verified. *Hin*dIII/*Mfe*I fragments were inserted into pAdlox modified by the addition of the EGFP coding sequence (pAdLoxGC3). Full-length EGFP-Scrib in pADlox was prepared by ligating the *Hin*dIII/*Rsr*II fragment from N-term Scrib and *Rsr*II/*Mfe*I fragment from pLK01 into *Hin*dIII/*Mfe*I digested pAdlox GC3 (#1, pLK49). EGFP-LRR/LAP was also cloned into the pShuttle vector [aa 1–420, pLK95, He et al., 1998]. N-terminal EGFP-Scrib deletion constructs, ΔLRR (aa 382–1630, pLK15) and ΔLRR/LAP (aa 421–1630, pLK17), were generated from a series of cloning steps. First, PCR products amplified using nAH60/nAH64 and nAH61/nAH64, respectively were digested with *Hin*dIII/*Bgl*II, cloned into pBSII SK (+) and sequenced. The *Hin*dIII/*Bgl*II fragments were subcloned into HA01022 to give ΔLRR, aa 382–1630, and ΔLRR/LAP, aa 421–1630. These altered Scrib constructs were first cloned into EGFP-C3 and then the EGFP-Scrib fusions were cloned into pAdLox. Plasmid DNAs were transformed into either DH10B or GeneHogs (Invitrogen).

Expression plasmids encoding hVangl2 and hVangl2Δ4 (hΔ4) were prepared by PCR using KIAA1215 as template with primer pairs nAH190/nAH191 and nAH190/nAH194, respectively. Products were cloned into pGEM T-Easy, sequence verified, and *Hin*dIII/*Mfe*I fragments subcloned into pAdLoxGC3. The expression plasmid encoding Lgl2 was amplified from IMAGE clone 5575350 with primer pairs nAH232/nAH233, cloned into pcDNA3.1-V5-His TOPO, and sequence verified. Two independent constructs were recovered with the following mutations: pAM9, L831P and pAM11, A566D and Q618K. The wild-type (WT) hLgl2 construct (pAM14) was obtained by subcloning the *Bsp*EI/*Not*I fragment from pAM11 into pAM9. All primer sequences are available upon request. Sequences of all plasmids were verified.

Recombinant adenoviruses were prepared using EGFP-Scrib constructs in the pAdlox shuttle vector with the Cre-lox system [Hardy, 1997]. EGFP-LRR/LAP in pShuttle (pLK95) was transformed into BJ 5183 cells with pADEasy-1 [He et al., 1998], recombinants selected and transfected into HEK293A cells to amplify the recombinant adenovirus.

To determine which Lgl genes were expressed in hepatic cells, we first identified human Lgl1 and mouse Lgl2 IMAGE clones (GI:5540713 and GI:1886537, respectively) through database searches. Restriction fragments from the Lgl clones were used as templates for preparation of the labeled random primed probes used in Northern analysis. Total RNA was extracted with TRIzol Reagent (Invitrogen) from freshly isolated hepatocytes, WIF-B, and Fao cells. To minimize variability in yields, mRNA was isolated from 0.5 to 1 mg total RNA using Oligotex according to the manufacturer's instructions (Qiagen) and used for Northern analysis or RT-PCR.

Isolated mRNA was resolved on a formaldehyde agarose gel then transferred to GeneScreen Plus membrane (NEN) using standard

techniques [Ausubel et al., 1995]. The blots were hybridized in [5× SSPE (20× SSPE: 3 M NaCl, 0.02 M EDTA, 0.2 M $NaPO_4$, pH7.4)/10% dextran sulfate/50% formamide/1% SDS/0.1% Ficoll/0.1% PVP40/0.1% BSA, 200 μg/ml salmon sperm DNA] at 45°C with either a random-labeled $^{32}$P-mouse Lgl1 or human-Lgl2 cDNA fragment. As an RNA loading control, blots were also hybridized with a random $^{32}$P-labeled rat GAPDH *Bxt*I/*Xho*I cDNA fragment (GI: 2671355). Final rinses were in 0.2× SSC (1× SSC: 0.15 M NaCl, 0.015 M sodium citrate)/0.1% SDS at 45°C and the membranes exposed to film at −80°C.

### Cell Culture, Transfection, Infection, and Immunofluorescence

Cre8 and HEK293A cells were cultured as recommended by the supplier. Fao and WIF-B cells were grown as previously described [Ihrke et al., 1993; Shanks et al., 1994]. Briefly, $10^6$ cells were plated either onto dishes (10 cm) directly or dishes containing 6 glass coverslips (22 × 22 mm) and fed every other day until use. MDCK cells (Strain II) were obtained from I. Mellman (Yale University, New Haven, CT) and cultured as described [Koivisto et al., 2001].

One day before transfection, HEK293A or MDCK cells were plated onto either duplicate 10 cm dishes containing a single coverslip to determine transfection efficiency (for biochemical assays) or coverslips in six-well cluster dishes (for immunofluorescence anaylsis). MDCK (all N-terminal constructs) or HEK293A (N-half and all PDZ constructs) cells were transfected with Effectene (Qiagen) according to the manufacturer's instructions using 2 μg or 0.4 μg of DNA for plates or coverslips, respectively, incubated with transfection reagents overnight, rinsed with fresh media and refed. HEK293A cells were also transfected with Lipofectamine (Invitrogen) according to the manufacturer's instructions using 3–6 μg DNA/10 cm dish. Approximately 16 (HEK293A cells) or 48 h (MDCK cells) post-transfection, cells were used for localization, biochemical studies, or pull-down assays. For adenovirus infection, MDCK cells were infected with $1.2–3 \times 10^9$ vp/ml in OPTIMEM (Invitrogen) (1 h), then rinsed with normal calcium containing medium (200 mg/L) and incubated (37°C) for the times indicated. Transfected MDCK cells stably expressing hLglV5-6His (pAM14) were selected with 400 μg/ml Geneticin.

For immunolocalization studies, WIF-B cells were seeded at $2 \times 10^4$ cells/cm$^2$ on glass coverslips and infected 8–11 days later when optimal polarity was established. Cells were rinsed with 1× HBSS and 100 μl of diluted virus ($1.2 \times 10^9$ to $2.0 \times 10^{10}$ vp/ml OptiMEM, Invitrogen) was applied to each coverslip. OptiMEM lacking virus was also applied to coverslips (uninfected control). After incubation (37°C, 1 h), the virus was removed, fresh medium added and the cells cultured for 16–20 h before analysis. For biochemical analysis, WIF-B cells were seeded at $5 \times 10^5$ cells /10 cm dish containing a single coverslip and infected as outlined above except that cells were co-infected with EGFP-Scrib viruses ($1.2 \times 10^9$ vp/ml) and either 1.4 or 2.9 × $10^9$ vp/ml of an empty virus (carrier virus) to achieve low and uniform expression of Scrib recombinant proteins.

For localization studies, cells plated on coverslips were rinsed briefly in PBS then fixed with 4% PFA (1 min) on ice and permeabilized with ice cold 100% methanol (10 min) and rehydrated in PBS (3 × 5 min) (Method A, [Mevel-Ninio and Weiss, 1981]). Subsequent incubations were at RT. Samples were blocked in 1% BSA/PBS (30 min), incubated in primary antibody (1 h), rinsed in PBS (3 × 5 min), then incubated with secondary antibody (1 h), rinsed in PBS (3 × 5 min), and mounted in 25% glycerol/2 mg/ml phenylenediamine in Tris buffered saline, pH 9.5–10.5 (TBS, 20 mM TRIS/149 mM NaCl). Primary and secondary antibodies were diluted in 1% BSA/PBS. Extracted samples were prepared essentially as described (Method B, [Araki et al., 1993]), except for the methanol fixation step. Briefly, cell were rinsed in PBS and extracted with 0.025% saponin in PHEM buffer, pH6.8 (60 mM PIPES/25 mM HEPES/10 mM EGTA/2 mM $MgCl_2$) (2 min). Samples were then rinsed in 0.025% saponin/PHEM/8% sucrose (2 × 2 min) and fixed in 4% PFA/8% sucrose/PBS (30 min), permeabilized with ice cold 100% methanol (10 min) and then rehydrated in PBS (3 × 5 min). The labeling steps were carried out as described above, except that the blocking and rinsing solutions contained 0.025% saponin. All incubations were performed at RT. Localizations were performed with the following primary antibodies: anti-Scribble, anti-E-cadherin, and anti-V5 (1:300, 1:1,000, 1:5,000, respectively). Appropriate secondary antibodies were used at 2–3 μg/ml.

The labeled cells were examined by epifluorescence (Zeiss Axioplan, Carl Zeiss, Germany) and digital images were collected with a Micromax CCD camera (Princeton Instruments, Trenton, NJ) using IPLab 3.5 software (Scanalytics, Fairfax, VA). Single plane confocal images were acquired with an Orca-ER CCD camera (Hamamatsu Photonics K.K., Hamamatsu City, Japan) and Ultraview 5.4 software in the Spatial Module (Perkin Elmer Life Sciences Division, Foster City, CA) using the Ultra View Confocal Imaging System equipped with the Nipkow spinning disc (Perkin Elmer Life Sciences Division). For co-localization analysis and to obtain color images, 12-bit files were merged in Photoshop 5.0 or 7.0.

### Biochemical Methods

For preparation of cytosol and membrane fractions, WIF-B or MDCK cells were scraped into buffer (0.25 M sucrose/3 mM imidazole, pH 7.4) containing protease inhibitors (1 mM PMSF, 1 mM benzamidine, 5 μg/ml antipain and leupeptin, 1 μg/ml pepstatin, 2 μg/ml aprotinin, 1 mM EDTA) and homogenized in a ball-bearing homogenizer (bore size, 0.25″, ball diameter, 0.249″). Cell lysis was monitored by phase microscopy using a 25× objective. Unbroken cells (representing 10–40% of the cell lysate) were sedimented (300*g*, 4°C, 10 min, Eppendorf 5402) and the resulting supernate centrifuged (100,000*g*, 4°C, 90 min, Beckman Optima TLX, TLA55) to yield a pellet containing all cellular membranes. The final pellet and supernates were analyzed by immunoblotting for the presence of either APN or E-cadherin, PM markers, and α-tubulin, a cytosolic marker.

For quantification of Scrib protein following transfection/infection, cells were scraped into SDS–PAGE sample buffer (10 mM Tris-HCl (pH 8.8)/2 mM EDTA/2.5% SDS/15% w/v sucrose), boiled (3 min) and the DNA sheared with a 28 or 27 g needle. Samples were reduced with 2-mercaptoethanol (10% v/v), boiled (3 min), separated by SDS–PAGE and transferred to 0.45 μm nitrocellulose (BA83, Schleicher and Schuell) for 4 h with 400 mA. Anti-APN, anti-E-cadherin, anti-Scribble, and anti-α-tubulin (1:2000, 1:1,000, 1:1,000, and 1:5,000, respectively) were diluted in 1% BSA, 0.1% Tween 20 and used for immunoblot analysis. Super Signal reagent (Pierce, Rockford, IL) was used according to the manufacturer's instructions. Chemiluminescence signals were initially captured with the Alpha Innotech (IMGEN Technologies, Alexandria, VA) or the Versa Doc (BioRad, Hercules, CA) imaging systems for quantitation.

### Assays of Protein–Protein Interactions

**BN–PAGE.** For BN–PAGE of whole cell extracts, low ionic strength buffers were used to preserve putative complexes [Tomita et al., 2005]. HEK293, MDCK, and WIF-B cells on 10 cm dishes were rinsed with PBS then scraped into 500 μl solubilization buffer (20 mM Tris, pH 7.0, 1.0% Triton X-100 with protease inhibitors, as above) giving a final volume of 600–700 μl. Cells were lysed by vortexing and homogenization with a 28 g needle then incubated (4°C, 30 min). Detergent concentrations were varied in order to achieve protein/detergent rations of 0.4–1.0. Following centrifugation (16,800*g*, 4°C, 10 min), supernatants were mixed in a 10:1 vol/vol ratio with loading buffer (5% wt/vol Coomassie Blue G250, 200 mM Bis-Tris, pH 7.0, 1 M 6-aminocaproic acid, 30% wt/vol sucrose) and loaded onto 5–13% gradient polyacrylamide gels with native markers as reported [Schagger, 2001]. Improved yields of the Scrib complex were achieved by the addition of SDS (1.0%) to the sample in lieu of loading buffer and heated (50°C, 10 min or 100°C, 3 min). BN–PAGE was performed at 4°C for 4–5 h as described [Schagger, 2001]. BN–PAGE gels were transferred (20% v/v methanol/0.1% SDS/25 mM TrisBase/192 mM glycine) to PVDF membranes for 4 h with 400 mA. Membranes were allowed to dry several hours, destained with 100% methanol for 10 min, then incubated in blocking solution (0.5% Casein/PBS, pH7.0), diluted primary antibodies (in 0.5% Casein/PBS, pH7.0/0.04% Tween) followed by secondary antibodies (in 0.5% Casein/PBS, pH7.0/0.01% Tween) and visualized as above.

To achieve better resolution of large molecular weight protein bands, soluble material (~2 mg of total protein as above) was layered onto 14–58% or 10–40% glycerol gradients (in 100 mM NaCl, 10 mM HEPES, pH7.4, 2 mM EDTA, 0.1% Triton X-100) [Greger et al., 2003; Tomita et al., 2005]. Refractive index was used to achieve designated glycerol concentrations. Gradients were prepared using an automated gradient maker (Biocomp) and centrifuged in an SW-41 rotor, 41,000 rpm (288,000*g*), 19 h, 4°C, slow acceleration and deceleration). Fractions (1.0–1.2 ml) were

collected using an automated pump (Buchler). Linearity of the gradients was determined by measuring the refractive index. Gradient fractions (60 μl) were mixed in a 10:1 vol/vol ratio with loading buffer and proteins separated by BN–PAGE as above or with SDS–PAGE sample buffer as above.

**Co-immunoprecipitation.** For pull-down of Lgl2-V5-6His by endogenous (endo) Scrib, anti-Scrib (2 μg) was added to 500 μl of indicated glycerol gradient fractions, incubated (4°C, ~4 h), then Protein G agarose beads were added and incubated (4°C, 2 h). Beads were washed with PBS/10% glycerol (3×) and the bound proteins eluted in SDS–PAGE sample buffer (as above). For pull-down of endo Scrib with Vangl2, MDCK cells (10 cm plate) were transfected with GFP-hVangl2 or GFP-h2Δ4 plasmids. Sixteen hours later, cells were washed once with PBS, scraped into KBO buffer (25 mM sodium phosphate, pH 7.4, 300 mM NaCl, 0.5% Triton X-100, 0.02 M octyl-glucoside, and 0.02% sodium azide) with protease inhibitors (as above), sheared with a 28 or 27 g needle and incubated (4°C, 60 min). Following centrifugation (100,000*g*, 4°C, 60 min, Beckman Optima TLX, TLA55), supernatants were incubated with anti-GFP antibody (0.2 μg, 4°C, ~16 h). Protein A agarose beads were added and incubated (4°C, 4 h). Beads were then washed with KB buffer (25 mM sodium phosphate, pH 7.4, 300 mM NaCl, 0.5% Triton X-100, and 0.02% sodium azide) (3×), TBS (50 mM Tris, pH 7.5, 100 mM NaCl) (2×) and the bound proteins eluted in SDS–PAGE sample buffer (as above).

HEK293A cells co-transfected with hLgl2-V5 and indicated Scrib plasmids, 16 h later were treated as outlined above except that the phosphatase inhibitors, 0.2 mM $NaVO_3$ and 50 mM NaF, were included. For pull-down of EGFP-Scrib by Lgl2-V5-6His, Anti-V5 (0.8 μg) was used and to pull-down Lgl2-V5-6His by EGFP-Scrib fusion proteins, anti-GFP (0.2 μg) was used. The detergent supernatant, unbound and bound fractions were analyzed by quantitative immunoblotting (anti-GFP from Molecular Probes and anti-V5 from Serotec, diluted 1:1,000 and 1:3,000, respectively) following SDS–PAGE and transfer to nitrocellulose.

**Peptide coupling.** C-terminal peptides of Vangl2 with the PDZ binding motif (PBM) (hVangl2, CEFVDPKSHKFVMRLQSETSV) and without the PBM (hΔ4, CEFVDPKSH KFVMRLQS) were synthesized with cysteine at their N-termini. Vangl2 peptides were bound to SulfoLink Coupling Gel (agarose beads) according to manufacturer's instructions. Briefly, following equilibration in coupling buffer (50 mM Tris, pH 8.0, 5 mM EDTA), peptides (2.5 mg/ml) were added to 1 ml of beads and incubated with end-over-end mixing (15 min) then without mixing (30 min). Unbound peptides were collected by centrifugation. Peptide-bound beads were washed with coupling buffer (1 ml, 3×) then unbound sites were blocked with 50 mM L-cysteine-HCl (1 ml). After washing with 1 M NaCl (1 ml, 6×) the beads were stored in PBS with 0.05% sodium azide at 4°C. Coupling efficiency was determined by comparing either the absorbance at 280 nM or the protein concentrations of the unbound fraction and starting fractions. As a control, cysteine coupled-beads were prepared using 50 mM L-cysteine-HCl (1 ml, 2×). All steps were performed at RT.

**Preparation of soluble EGFP-Scrib fusion proteins.** GFP-Scrib fusion proteins were expressed in HEK293A cells following either transfection with Effectene (EGFP-N-half and EGFP-PDZs 1–4, 1–2, 2–3, 3–4 plasmids) or recombinant adenovirus infection (EGFP-95-1630 and EGFP-C-half). After ~16 h, the cells were rinsed in PBS and lysed in KBO buffer containing protease inhibitors (as above). DNA was sheared with a 27 g needle, extracts incubated (4°C, 30 min) and centrifuged (100,000*g*, 4°C, 90 min, Beckman Optima TLX, TLA55) to yield a supernatant containing soluble EGFP-Scrib fusion proteins. Before pull-down studies were performed, levels of soluble proteins were determined by immunoblot analysis using anti-GFP. Equivalent amounts of each protein were then used.

**Vangl2 pull-down assay.** hVangl2, hΔ4, or cysteine-coupled agarose beads were incubated (1 h) with BSA (2 mg/ml) in TBS + 1 mM PMSF with end-over-end mixing to bind non-specific protein binding sites and then washed (4×) with binding buffer (50 mM Tris,7.5, 100 mM NaCl, 0.1% NP40, 1 mM PMSF). Beads (50 μl of a 1:1 slurry) and equalivalent amounts of EGFP-Scrib fusion proteins were combined in 400 μl binding buffer with 2 mg/ml BSA. Samples were incubated (1 h) with end-over-end mixing, washed with binding buffer (1 ml, 3×) then with TBS + 1 mM PMSF (1 ml, 2×). All steps were performed at RT. SDS–PAGE sample buffer (1×) was added to the beads, proteins

were separated by SDS–PAGE and transferred to nitrocellulose for immunoblotting.

## RESULTS

For our studies, we chose polarized MDCK and hepatic WIF-B cells [Ihrke et al., 1993; Shanks et al., 1994] in order to examine Scrib's behavior in epithelial cells with two different morphologies. In contrast to the simple columnar morphology of MDCK cells, hepatocytes are polygonal cells with at least two basal surfaces in contact with the blood and multiple apical surfaces forming the bile canaliculus, a branched network of grooves between adjacent cells [Hubbard et al., 1994]. In both cell types, endo Scrib localized to the basolateral surface (Fig. 1B, WIF-B cells), as did exogenous Scrib, which we tagged with an N-terminal EGFP (Fig. 1A,C). A similar construct was shown to complement Scrib mutant flies [Dow et al., 2003]. Using a simple fractionation scheme to separate cytosol from membranes in WIF-B and MDCK cell homogenates, we found most of the endo Scrib and a majority of the EGFP-Scrib present in the high speed pellet fractions (Fig. 1D,E). Based on these intital results, we concluded that EGFP-Scrib fusions were valid reporters of Scrib's PM association in both cell types. Therefore, we generated an array of EGFP-Scrib mutants and used morphological and biochemical approaches to identify the domain(s) of Scrib responsible for this association.

### The LRR Domain Mediates Scrib's Localization at the Basolateral PM

A single point mutation in the LRR domain was reported to disrupt Scrib's PM localization in MDCK cells [Legouis et al., 2003], prompting us to ask if LRR alone could associate with the membrane. The first four mutants we studied contained LRR alone or with increasing amounts of C-terminal sequence (Fig. 2A). Our analysis of WIF-B cells was limited, because of difficulty in generating recombinant adenoviruses encoding the LRR. However, when transfected into MDCK cells, all constructs expressed EGFP-fusion proteins of the predicted sizes (Fig. 2B). Biochemically, we found that the two shorter LRR-containing proteins (GFP-LRR and GFP-LRR/LAP) distributed with the membrane fraction to a greater extent than did the two longer LRR proteins (Fig. 2C).

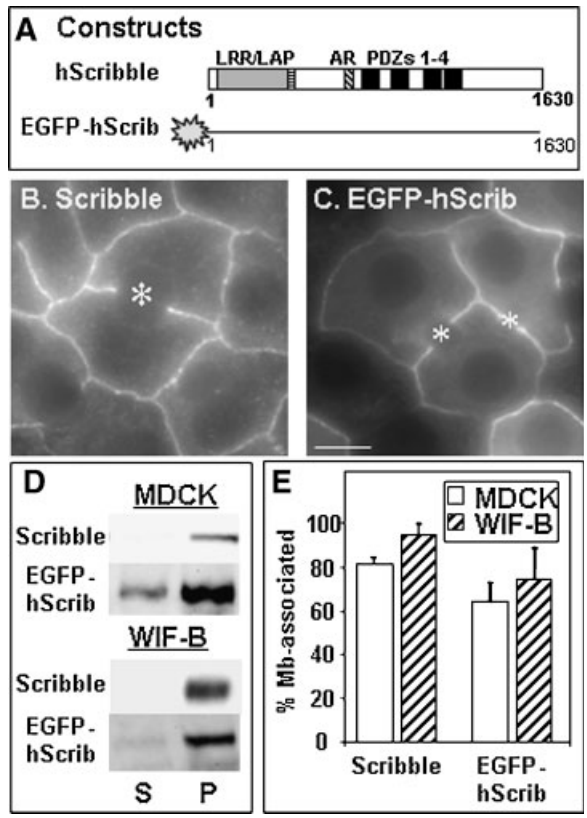


**Fig. 1.** Endogenous and exogenous Scrib localize to the basolateral PM of polarized cells. **A**: Domain organization of Scribble: aa13-381=LRR, aa381-420 = LAP, aa659-723 = AR (Acidic Region), aa 726-1202 = PDZ domains. **B**, **C**: Morphological localization of full-length Scrib. Mature WIF-B cells were fixed (Method A, M and M) and stained with anti-Scrib antibody. **C**: WIF-B cells were infected with EGFP-Scrib adenovirus and the GFP distribution examined following fixation (Method A). Asterisks indicate the location of apical cysts in WIF-B cells. Bar = 10 μm. **D**: Immunoblot analysis of full-length Scrib. In WIF-B and MDCK cells, endo Scrib associated overwhelmingly with the membrane fraction, EGFP-Scrib showed a similar distribution in WIF-B cells while in MDCK cells, slightly less was present. The cytosol (S) and membrane (P) fractions can be directly compared, since the same relative amounts of each fraction were loaded onto SDS–PAGE. For all fractionation studies, the distributions of tubulin and E-cadherin in S and P were quantitated by immunoblot and found to be >80% cytosolic (tubulin) or membrane (E-cadherin). **E**: Quantitation of Scrib at the PM. Blots were used to calculate the % Mb-associated Scrib. The signal intensity in P (HSP) was divided by the sum of the intensities in P and S (HSS) X 100. Standard deviations (SD) are shown when three to five determinations were obtained.

In fact, ~70% of the LRR-only protein was membrane-associated, when its distribution was normalized to that of EGFP-Scrib. We observed GFP fluorescence of each fusion protein at the basolateral PM of transfected MDCK cells (Fig. 2D,E, constructs #2 and #5 are

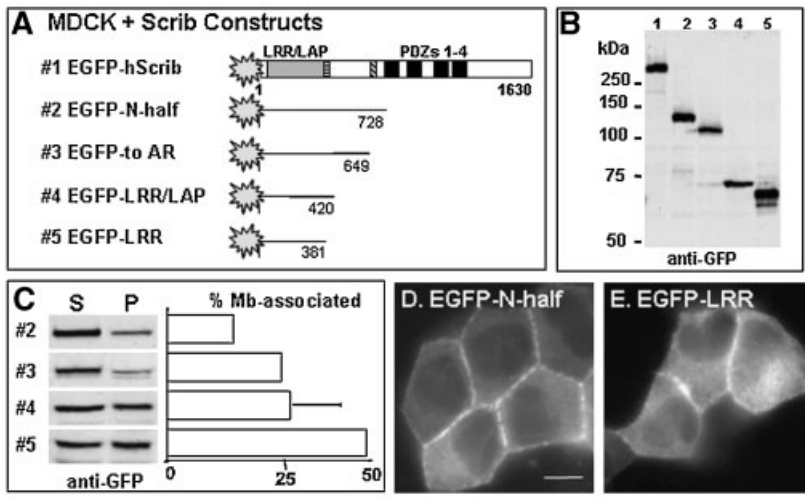


**Fig. 2.** The LRR domain of Scrib associates with membranes of MDCK cells. **A**: EGFP-Scrib constructs 1–5 were transfected into MDCK cells (efficiencies 3–8%). **B**: The SDS–PAGE mobilities of exogenous EGFP-Scrib proteins 1–5 were determined by anti-GFP immunoblotting of cell extracts and were consistent with expression of intact fusion proteins. **C**: Twenty-four hours after transfection, cytosol (S) and membrane (P) fractions were prepared from cell extracts then analyzed by SDS–PAGE and anti-GFP immunoblotting and the % Mb-associated Scrib calculated as for Figure 1E. Values are the average of two determinations except for construct #4 where the SD is shown. Recombinant adenovirus encoding construct #4 when expressed in WIF-B cells exhibited 13 % Mb-associated (N = 1). **D**, **E**: GFP fluorescence corresponding to the total cellular pools of EGFP-Scrib fusion proteins N-half (**D**) and LRR (**E**) are shown. Bar = 10 μm.

shown). In WIF-B cells, the LRR/LAP protein was also found at the basolateral PM, both biochemically (~13%) and morphologically (data not shown), but to lesser extents than in MDCK cells. Nonetheless, the results clearly showed that the LRR domain was capable of associating with the PM independently of other Scrib domains and the LRR alone bound nearly as well as full-length Scrib in MDCK cells.

### The PDZ Domains Also Mediate Scrib's Localization at the Basolateral PM

We next asked if N-terminal deletions of Scrib would disrupt the protein's association with the PM. Given published images of a cytoplasmic localization of full-length Scrib bearing the single point mutation P305L in the LRR domain, we were initially surprised that EGFP-Scrib encoding aa 95–1630, which is missing the first three and a half LRR repeats, still localized to the PM of MDCK and WIF-B cells (data not shown). When cells were fractionated, ~45% and ~30% of the LRR mutant protein distributed in the membrane fraction of MDCK and WIF-B cells, respectively (Fig. 3A,B, construct #6). Again, normalizing these levels to those of the EGFP-Scrib full-length standard indicated that ~70% and ~40% of truncated EGFP-Scrib associated with the membrane fraction in MDCK and WIF-B cells, respectively. Two additional N-terminal truncations, ΔLRR and ΔLRR/LAP also showed membrane association, although at reduced levels (Fig. 3B, constructs #7 and #8, respectively).

To determine which region contributed to the reproducible PM association in constructs lacking the complete LRR domain, we generated constructs encoding only domains in the C-terminal half of Scrib (Fig. 3A). Fractionation of homogenates from transfected/infected cells revealed that the EGFP-C-half and EGFP-PDZ 1–4 proteins associated with the membrane (Fig. 3B constructs #9 and 10, respectively); however, Scrib protein consisting of the C-terminal 433 aa bound very poorly (Fig. 3B construct #11).

Fluorescence images confirmed the biochemical findings (Fig. 3C). EGFP-C-half was localized to the PM and cytosol in WIF-B cells, as well as to the TJ when cells were fixed with paraformaldehyde and permeabilized with methanol (Total, Fig. 3C). The PM and TJ associations were even more apparent when the cells were first extracted with 0.025% Saponin and then fixed with paraformaldehyde (Extracted, Fig. 3C). The TJ association of EGFP-Scrib proteins was variably observed while endo Scrib was never observed at the TJ. In MDCK cells, EGFP-C-half gave similar results, except that the ectopic mutant EGFP-

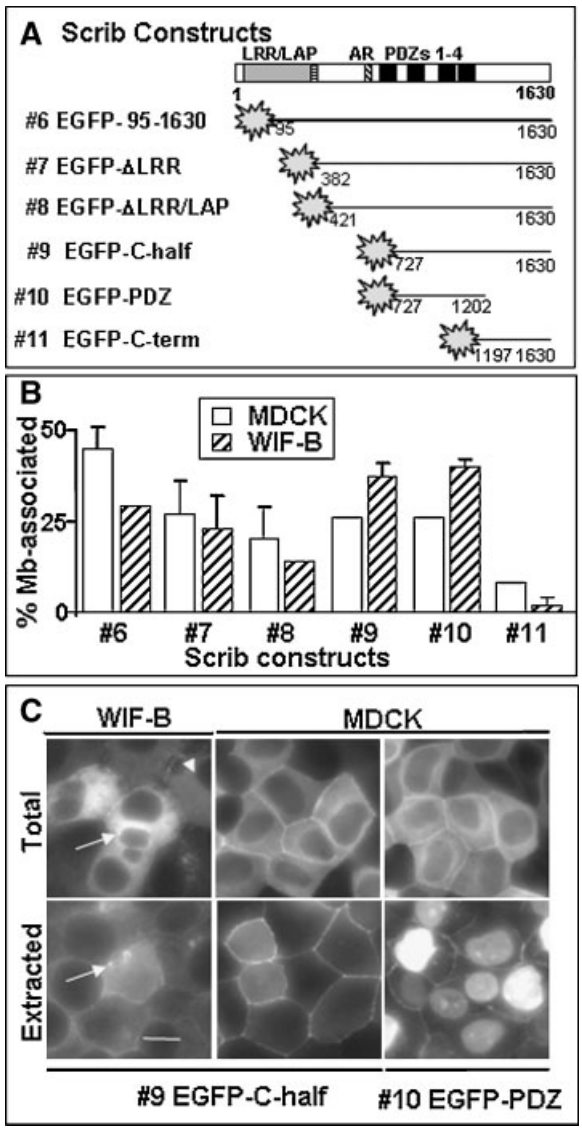


**Fig. 3.** The PDZ domain of Scrib associates with membranes of MDCK and WIF-B cells. **A**: Cells were infected with EGFP-Scrib adenoviral constructs #6–11. Fractions were prepared and analyzed as described in Figure 1. **B**: Quantitation of Scrib fusion proteins at the PM of polarized cells. The % Mb-associated Scrib is calculated as described in Figure 1E. Values for Constructs #10 and #11 in WIF-B cells are from one determination. **C**: GFP fluorescence in cells was examined after fixation using Method A (see M and M), which reveals the total cellular EGFP-protein signal, or Method B, which extracts the soluble EGFP-protein and retains the membrane-associated signal. In images of EGFP-C-half protein at the basolateral PM and TJ in WIF-B cells, the arrow indicates TJ in cross-section and arrrowhead shows the TJ belt or ring encircling the apical surface [Ihrke et al., 1993]. For MDCK cells, images were captured at the level of the nucleus.

Scrib proteins did not localize at the TJ. While biochemically the EGFP-C-half (construct #9) and the EGFP-PDZ (construct #10) gave similar results (Fig. 3B), we routinely observed a stronger GFP signal from the EGFP-C-half protein at the PM following extraction (MDCK, Fig. 3C). We conclude that the PDZ domains of Scrib can associate with the PM independent of other domains and addition of the C-terminal domain may stabilize this association.

### Scrib Associates Biochemically With the Polarity Protein, Lgl2.

Genetic studies in Drosophila linking Scrib and Lgl [Bilder et al., 2003; Tanentzapf and Tepass, 2003] prompted us to ask if the two proteins interacted biochemically in mammalian cells. Of the four human Lgl genes [Katoh and Katoh, 2004], Lgl1 and Lgl2 are the best studied to date [Musch et al., 2002; Yamanaka et al., 2003]. Lgl1 is widely expressed while Lgl2 has a more restricted expression pattern in mouse tissues (Fig. S1A). As both Lgl1 and Lgl2 were present in extracts of whole liver, which is composed of multiple cell types, we examined their expression in freshly isolated rat hepatocytes as well as cultured cells. Only Lgl2 was present in hepatocytes while both were present in the cultured cells (Fig. S1C).

Because Lgl2 expression was abundant in kidney, we used MDCK cells to test for a biochemical link between Scrib and Lgl2. Detergent extracts of MDCK cells were separated on 10–40% glycerol gradients and fractions analyzed by BN–PAGE, which has been used recently to identify multimeric protein complexes in mammalian cells [Yang et al., 2002; Tomita et al., 2005]. Separated proteins were transferred to PVDF membranes then analyzed by immunoblotting (Fig. 4A). We often observed Scrib as several broad smears of immunoreactive material with increasing sizes in sequential fractions of the gradient (Fig. 4A, lanes 4, 5, 6, and 7) suggesting that the protein might be in multiple complexes. The finding that more Scrib was detected in BN-gels following SDS treatment of MDCK cell lysates strengthened the idea that Scrib was in large complexes (Fig. S2A). In fact, Scrib was only detected in hepatic cells after the addition of SDS (Fig. S2A). SDS-treated Scrib migrated with an apparent molecular mass more than twice its predicted value, 182 kDa, a finding consistent with previous reports [Lee et al., 2002; Greger et al., 2003; Tomita et al., 2005]. Importantly, by SDS–PAGE, a significant amount of endo Lgl2 was found to co-migrate

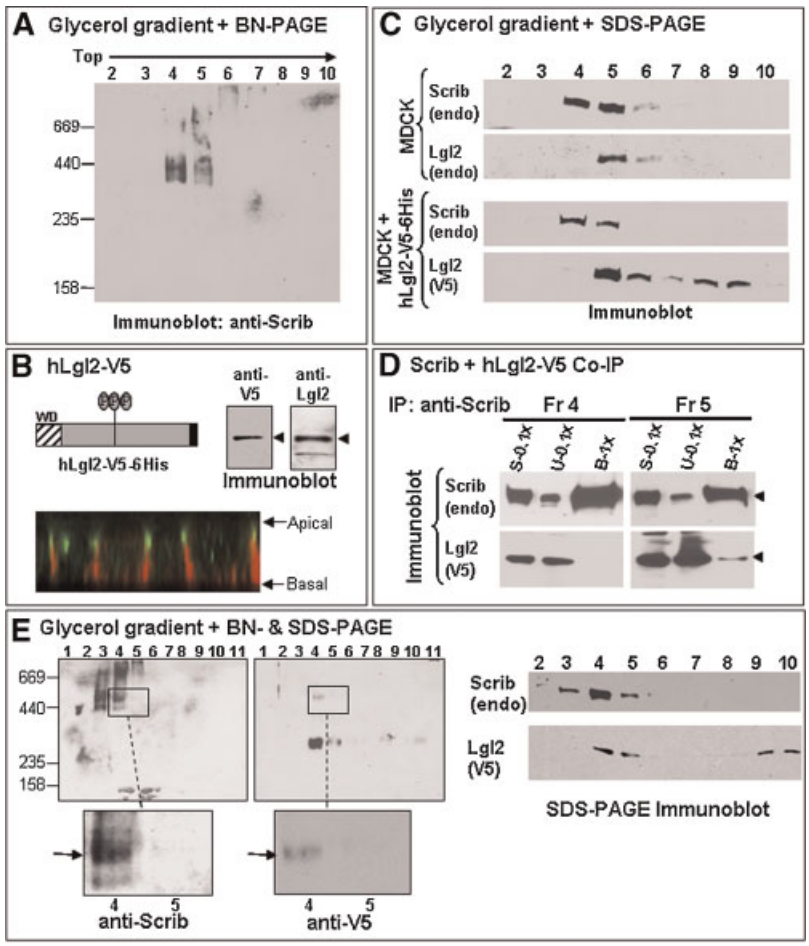


**Fig. 4.** Identification of a Scrib complex and Lgl2 association by BN–PAGE. **A**: Identification of the Scrib complex. Triton X-100 lysates of MDCK cells (grown for 5 days on a 10 cm dish) were separated on a 10–40% glycerol gradient, 6 µl of 10× sample buffer was added to 60 µl of fractions (1 ml), resolved by BN–PAGE on a 5–13% Bis-Tris gradient gel and analyzed by immunoblotting with anti-Scrib. Markers are: thyroglobin, ferritin, catalase, and aldolase designated 669, 440, 235, and 158 kDa, respectively. **B**: Lgl2 domain organization, which includes four WD-40 domains identified by Psi Blast (aa 5–35, 55–91, 103–151, and 163–192), three serine phosphorylation sites are indicated (P, aa 649, 653, and 660 are phosphorylated by aPKC [Yamanaka et al., 2003]), and a V5-6His epitope tag at the C-terminus (black box, 45aa). hLgl2-V5-6His-stably-transfected MDCK cells were fixed and stained with anti-V5 and anti-ZO-1. Confocal images (x–z sections) show hLglV5 (red) at the lateral PM and ZO-1 (green) at the TJ. Lysates from MDCK cells expressing Lgl2-V5-6His were separated on a 10–40% glycerol gradient, fraction 5 was analyzed by SDS–PAGE followed by immunoblotting as indicated. **C**: Endo and exogenous Lgl2 co-migrate with Scrib in glycerol gradients. Samples prepared from either MDCK or Lgl2 stable MDCK cell lines were analyzed by SDS–PAGE followed by immunoblotting as indicated. **D**: Co-immunoprecipitation of Scrib and Lgl2. Gradient fractions (500 µl) from (C) were used for IP with anti-Scrib and analyzed by SDS–PAGE and immunoblotting as indicated. S-0.1×, U-0.1× and B-1× = start, unbound and bound, respectively. **E**: BN–PAGE analysis of Lgl2 and Scrib complex. Lysates from MDCK cells expressing Lgl2-V5-6His were separated on a 10–40% glycerol gradient, fractions were resolved by BN–PAGE and SDS–PAGE in parallel and analyzed by immunoblotting as indicated. [Color figure can be viewed in the online issue, which is available at www.interscience.wiley.com.]

with Scrib in fraction 5 of the glycerol gradient (Fig. 4C, lane 5).

Because we could not detect endo Lgl2 by BN–PAGE, we prepared MDCK cells stably expressing a cDNA encoding human Lgl2 with a C-terminal epitope (hLgl2-V5-6His, Fig. 4B). A protein of the correct size was detected with both anti-V5 and our anti-Lgl2 (Fig. 4B). Like endo Lgl2 [Yamanaka et al., 2003], the protein was found at the basolateral surface and importantly for our analysis, not in inclusion bodies (Fig. 4B). Glycerol gradient analysis of these cells revealed that both Scrib and Lgl2 behaved as in non-transfected MDCK cells (Fig. 4C). Fractions from the glycerol gradient were analyzed by co-immunoprecipitation, which revealed a small but reproducible fraction of Lgl2-V5-6His associating with endo Scrib

(Fig. 4D). To study the native Scrib/Lgl2 complex further, we analyzed glycerol gradient fractions in BN gels by immunoblotting. When the membranes were incubated sequentially with anti-Scrib then anti-V5, we found two bands of Lgl2, one that co-migrated with Scrib at ~480 kDa, and the second migrating at ~240 kDa (Fig. 4E, lanes 4 and 5). Interestingly, the ~240 kDa Lgl2 was found throughout the gradient suggesting that during BN–PAGE it dissociated from larger complexes. The co-IP and BN–PAGE results, taken together, show that small amounts of Lgl2 associated with Scrib.

The analysis presented above indicated that Scrib was in multiple complexes; however, we were unable to assign molecular weights to them. Gradient fractions containing Scrib had densities of 1.0380–1.0621 g/cm$^3$, which are lower than that of purified proteins (i.e., 1.35 g/cm$^3$, [Quillin and Matthews, 2000]), suggestive of the presence of lipids present in the complexes. Moreover, Scrib migrated as broad smears in the BN gels and its mobility relative to the markers varied somewhat (compare Fig. 4A, lanes 4, 5, 6, and 7 and Fig. 4E, lanes 3, 4, and 5). Incomplete exchange of Coomassie Blue for the detergent and lipids could have contributed to the variability.

### The LRR Domain of Scrib Binds Lgl2

We next mapped the domain of Scrib that associated with Lgl2. HEK293A cells were co-transfected with hLgl2-V5-6His and various EGFP-Scrib constructs followed by co-immunoprecipitation and blotting. Quantitative immunoprecipitation was achieved with anti-V5 (Fig. S2B). A small but reproducible amount of full-length Lgl2 co-immunoprecipitated with full-length Scrib (Figs. S2B, 5A,B). Further, the N-terminal half of Scrib bound Lgl2, but the C-terminal half did not (Figs. 5B,S2B). Analysis of additional deletion constructs pointed to the LRR domain as the possible Lgl2 interaction domain on Scrib. Therefore, we tested three additional EGFP-Scrib fusion proteins and found that Lgl2 associated with all fusion proteins containing an intact LRR domain (Fig. 5B, constructs #4 and #5 are shown).

Next, we examined whether Scrib's LRR domain associated with Lgl2 in polarized cells and whether this association occurred at the membrane, in the cytosol or both. Co-expression of hLgl2-V5-6His and EGFP-LRR/LAP in

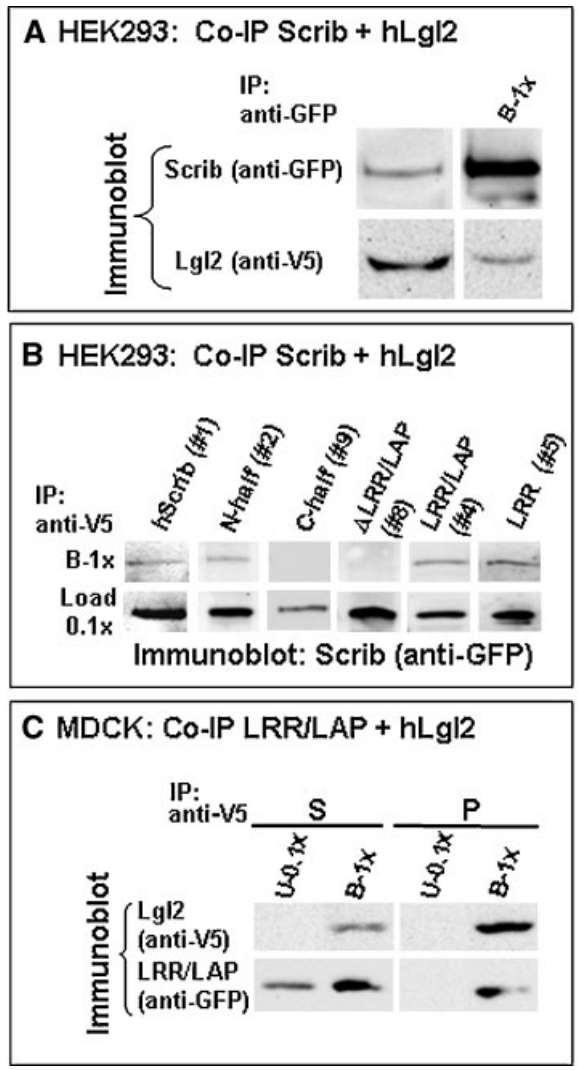


**Fig. 5.** The LRR domain of Scrib associates with Lgl2. **A**: Co-IP of exogenous Lgl2 and Scrib. HEK293A cells were co-transfected with hLgl2-V5-6His and EGFP-Scrib construct, extracts subjected to immunoprecipitation with anti-GFP and resulting fraction analyzed by SDS–PAGE and immunoblotting with anti-V5 showing Lgl2 co-immunoprecipitates with GFP-Scrib, 80% of the Scrib and ~1.5% of the Lgl was found in the bound fraction. **B**: Co-IP of exogenous Lgl2 and Scrib. HEK293A cells were treated as in B except that immunoprecipitations were performed with anti-V5 and resulting fractions analyzed by SDS–PAGE and immunoblotting with anti-GFP. Quantitative immunoprecipitation of Lgl resulted in $1.4 \pm 0.8$ of the total recovered Scrib (sum of bound and unbound material) in the bound fraction. Each example shown in B is representative of at least three determinations. **C**: The S and P fractions were prepared from MDCK cells co-expressing LRR/LAP and hLgl2, detergent extracted, and supernatants subjected to immunoprecipitation with anti-V5 and the resulting samples analyzed by SDS–PAGE and immunoblotting with the indicated antibodies. U-0.1× and B-1× = unbound and bound, respectively.

MDCK cells followed by subcellular fractionation indicated that ~90% of hLgl was associated with membranes (Fig. S2C). Moreover, the distribution of EGFP-LRR/LAP between the cytosol and crude membrane fraction was not altered by over expression of Lgl2 (Fig. S2C). Quantitative immunoprecipitation of Lgl2 in the membrane fraction brought with it all of the membrane-associated GFP-Scrib protein. Interestingly, the small but detectable amount of exogenous hLgl2 in the cytosol was also complexed with exogenous EGFP-LRR/LAP (Fig. 5C). These results indicate that exogenously expressed Scrib and Lgl2 can interact in either location.

### The PM Protein, Vangl2, Localizes to the Basolateral PM and Binds the PDZ Domains of Scrib

Genetic studies in mice linking the four-transmembrane protein Vangl2 with Scrib [Murdoch et al., 2001], prompted us to ask if these two proteins interact biochemically. Vangl1 and Vangl2 are 75% homologous and terminate in identical Type I sequence motifs that bind PDZ domains. Database searches and in situ hybridization revealed that both genes are widely expressed in mammals, with Vangl2 present in a large number of epithelial cell types. For the present studies, we generated constructs encoding a human Vangl2 fused to EGFP (EGFP-hVangl2) with and without its PDZ domain-binding motif (EGFP-hΔ4, Fig. 6A). Following transient expression in MDCK cells, we found EGFP-hVangl2 and endo Scrib at the basolateral PM as well as some EGFP-hVangl2 in vesicles below the apical surface (Fig. 6B). The distribution of EGFP-hΔ4 was similar, although less of the mutant seemed to be at the PM (Fig. 6C). When EGFP-hVangl2 and EGFP-hΔ4 fusion proteins expressed in transfected MDCK cells were quantitatively immunoprecipitated with anti-GFP, a small (2%) but reproducible amount of total endo Scrib was found in the full-length hVangl2 immunoprecipitate (Fig. 6D). In contrast, the mutant Vangl2 immunoprecipitate contained less than 0.1% of endo Scrib. Since only ~5% of the MDCK cells in the transiently-transfected population expressed EGFP-hVangl2, association of 2% of total Scrib with full length Vangl2 represented a substantial fraction, ~40%, of the endo Scrib in the transfected cells. As a specificity control, we

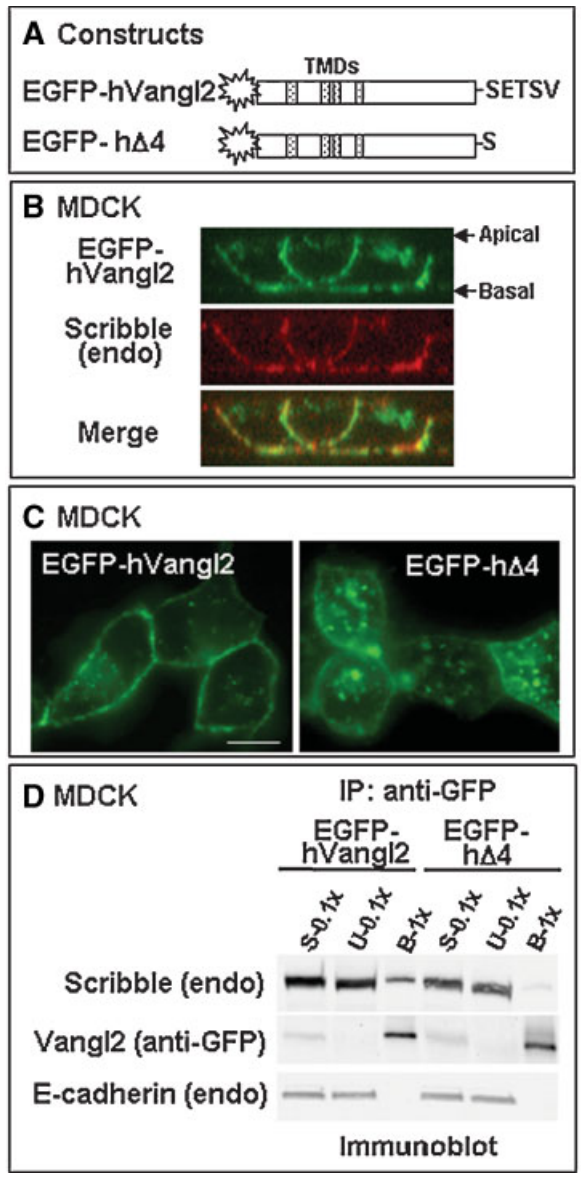


**Fig. 6.** Endogenous Scrib binds hVangl2 but not hΔ4. **A**: EGFP-hVangl2 and EGFP-hΔ4 domain organization. EGFP-hΔ4 lacks the 4 C-terminal residues, ETSV. TMD = transmembrane domains (stippled). **B**: EGFP-Vangl2 localizes to the basolateral surface of MDCK cells. Cells grown on glass coverslips were transfected with EGFP-hVangl2 and fixed 48 h later. Confocal images (x–z sections) show endo Scrib (red) and EGFP-hVangl2 at the basolateral PM. **C**: Both EGFP-Vangl2 and EGFP-hΔ4 exhibited similar expression patterns at the PM and in intracellular vesicles. Cells were transfected as for B. **D**: Co-IP of EGFP-Vangl2 and Scrib. Extracts of MDCK cells transfected with EGFP-hVangl2 or EGFP-hΔ4 construct were immunoprecipitated with anti-GFP, analyzed by SDS–PAGE and immunoblotting with the indicated antibodies. S-0.1×, U-0.1×, and B-1× = start, unbound and bound, respectively. [Color figure can be viewed in the online issue, which is available at www.interscience.wiley. com.]

determined that E-cadherin, an adherens junction protein found at the basolateral surface, did not co-immunoprecipitate with EGFP-hVangl2 (Fig. 6D).

To further define the domain of Scrib that bound Vangl2, we synthesized two peptides, hVangl2 with the C-terminal 20 aas and hΔ4, a mutant lacking the last four aas, coupled them to agarose beads and used them to pull-down different EGFP-Scrib constructs from transfected HEK293A cells (Fig. 6A). Only two constructs, EGFP-95-1630 and EGFP-PDZ 1–4, bound the hVangl2 peptide; constructs lacking the 4 PDZs failed to bind (Fig. 7A). We generated four additional constructs encoding various combinations of the four PDZ domains and found PDZs two and three together bound Vangl2 as well as all four PDZs and better than the other combinations (Fig. 7A). To determine whether the Scrib/Vangl2 association was direct, we used the peptide coupled beads to pull-down EGFP-95-1630 from HEK293A cell extracts. Examination by Coomassie Blue staining of the proteins bound to the hVangl2 and hΔ4 peptides showed clearly that EGFP-Scrib was the most intensely stained protein in the hVangl2 peptide bound lane (Fig. 7B). These results suggested that Vangl2 directly bound Scrib.

We examined the interaction of endo Scrib with the hVangl2 and hΔ4 peptides. After incubating the beads with HEK293A extracts, we probed for the presence of Scrib. Endo Scrib was bound to hVangl2 peptide beads but not the hΔ4 peptide (Fig. 7C). Because Strabismus, the Vangl homolog in flies (trilobite in zebrafish, [Sepich et al., 2000; Jessen et al., 2002; Jessen and Solnica-Krezel, 2004]) was reported to bind the PDZ protein, SAP97/Discs large 1 (Dlg1), [Lee et al., 2003], we examined the interaction of

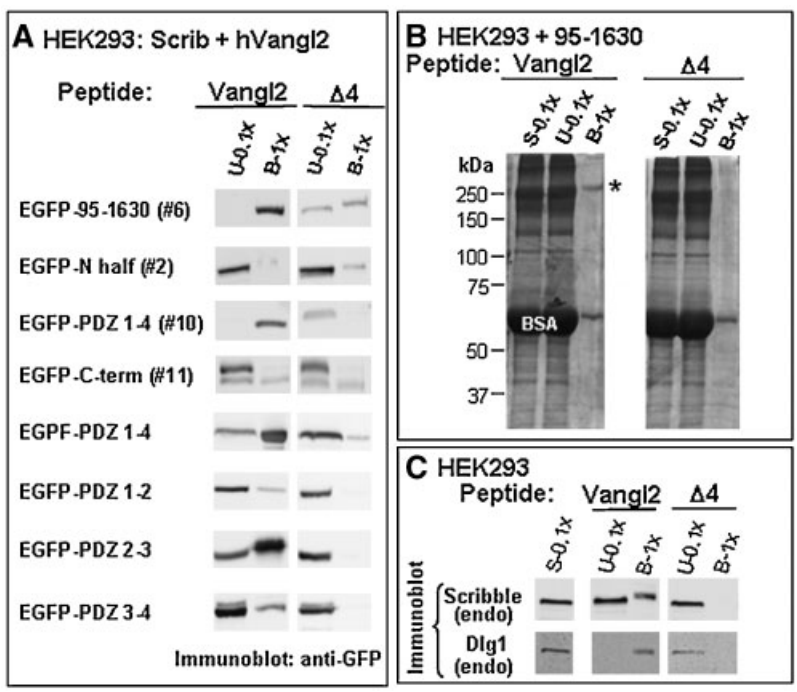


**Fig. 7.** The PDZ domains of Scrib bind Vangl2. **A**: Scrib/Vangl2 peptide bead binding assay. HEK293 cells were transfected with EGFP-Scrib constructs, cell extracts prepared, and fusion protein levels determined by immunoblot analysis. Extracts with equivalent amounts of fusion proteins were then incubated (1 h) with Vangl2, Δ4 peptide or cysteine-beads (data not shown), the beads washed and start (data not shown), unbound (U-0.1×) and bound (B-1×) proteins analyzed by SDS–PAGE and immunoblotting with anti-GFP. A non-specific band was detected by anti-GFP when blotting for expression of EGFP-C-term (#11). Amino acids in PDZ constructs are: PDZ 1–4, 727–1202; PDZ 1–2, 720–960; PDZ 2–3, 816–1114; PDZ 3–4, 962–1202. **B**: A Coomassie Blue stained SDS–PAGE gel from a pull-down assay in which Vangl2 or Δ4 peptide beads were mixed with extracts from HEK293A cells transiently transfected with EGFP-95-1630. Scrib (asterisk) was the only cellular polypeptide detected in the bound fraction when Vangl2 peptide beads were used. Bovine serum albumin (BSA), added as blocker, was also present. **C**: Vangl2 or hΔ4 beads were incubated (1 h) with HEK293A extract (S-0.1×) and washed. Bound (B-1×) and unbound (U-0.1×) proteins were analyzed by SDS–PAGE and immunoblotted with the indicated antibodies. Levels of endo Dlg were at the threshold of detection with anti-Dlg.

Dlg1 with Vangl2 peptide beads. Endo Dlg also bound hVangl2 peptide and not the hΔ4 peptide beads, demonstrating that the Vangl C-terminus bound multiple partners (Fig. 7C).

## DISCUSSION

Using systematic morphological and biochemical analyses of multiple EGFP-Scrib fusion proteins, we determined that the LRR and PDZ domains independently associate with the basolateral PM in two types of polarized mammalian epithelial cells. These results confirm and extend those recently reported for mammals [Navarro et al., 2005] and flies [Albertson et al., 2004; Zeitler et al., 2004]. Our biochemical studies identified several Scrib complexes in mammalian epithelial cells. While genetic studies indicate an interaction between Scrib and the cytoplasmic protein, Lgl, we documented this association biochemically using velocity gradient centrifugation combined with BN–PAGE analysis of the fractions. Further we identified the LRR domain of Scrib responsible for binding to Lgl2. Finally, we demonstrated for the first time that the membrane protein Vangl2 binds Scrib through a specific interaction with the latter's PDZ domains 2 and 3. Figure 8 summarizes the Scrib interactions identified to date, although their spatial and temporal associations remain to be determined.

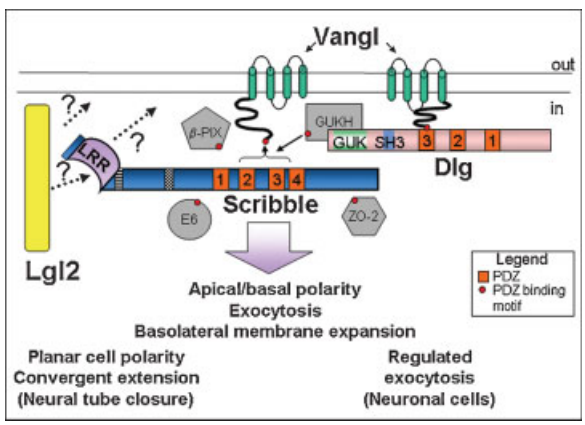


**Fig. 8.** A drawing of Scribble's binding partners and proposed biological roles. Our biochemical studies show that Vangl2 binds both Scrib and Dlg via the PBM (red dot). Scrib has multiple cytoplasmic binding partners including Lgl (this report), betaPIX [Audebert et al., 2004], HPV-E6 protein [Nakagawa and Huibregtse, 2000], and GUKH [Mathew et al., 2002]. As yet unknown for Lgl2 (dotted arrows) are: (1) the intracellular site of its binding to Scrib (membrane or cytosol); (2) the molecular domain that binds Scrib's LRR domain; and (3) its PM binding site/partner when Scrib is absent. Also unknown is whether the LRR domain of Scrib binds the PM directly or indirectly (dotted arrow). Proteins studied in this report are in color. [Color figure can be viewed in the online issue, which is available at www.interscience.wiley.com.]

### Scrib Has Multiple Cytoplasmic Binding Partners

Results of the biochemical approach we took in this study confirmed genetic data indicating an association between Lgl and Scrib. Although we do not yet know if this association is direct or indirect, docking of either or both proteins at the PM appears not to be essential for their interaction, since we were able to co-immunoprecipitate them from cytosolic and membrane fractions. However, Lgl can associate with the PM independently of Scrib, since loss of Dlg in flies leads to a partial loss of Lgl at the PM, while Scrib is totally dissociated [Roche et al., 2002]. Additionally, yeast has two Lgl homologs (SRO7 and SRO77) and no Scribble family members, implying the existence of additional binding partners for SRO7/77's role in yeast vesicle trafficking [Lehman et al., 1999].

A significant finding of this study was that Lgl2 associated with Scrib's LRR domain. Crystal structures of proteins with LRR domains consistently show a horseshoe shape with various radii (e.g., [Kobe and Deisenhofer, 1993, 1995, 1996; Kobe and Kajava, 2001; Kajava and Kobe, 2002; Enkhbayar et al., 2004]). Structural modeling of the LRR domain of C. elegans LAP protein, LET413, also best fit a horseshoe structure [Legouis et al., 2003]. LRR domains have also been co-crystalized with their protein ligands, showing very clearly that the latter bind to the concave face (inside) of the horseshoe [Enkhbayar et al., 2004]. By extension, Lgl2 most likely binds the same way. However, the orientation of the LRR structure at the PM is currently unknown. Can a second ligand bind on the outer face of the LRR structure? Since studies in flies suggest that Scrib recruits Lgl2 to the PM [Bilder et al., 2000], the outer surface of the LRR could associate with the PM either directly or indirectly and recruit, anchor or stabilize Lgl2 on its concave surface. This idea is consistent with findings in which a P to L mutation found on an external helix of Scrib's LRR disrupted its association with the PM [Legouis et al., 2003].

The new biochemical approaches used in this study provide evidence that Scrib is part of a macromolecular complex. Although Scrib complexes could be solubilized from tissue culture

cells with 1% Triton X-100, only 1% Empigen was able to release the protein from rat liver PM sheets (P. Tuma, unpublished data). Because of these biochemical properties, we speculate that Scrib may organize the intracellular face of the lateral PM in polarized epithelial cells and envision it playing predominantly a structural role, possibly serving as a "retaining wall." To document the Scrib/Lgl2 association, we used velocity gradient centrifugation combined with BN–PAGE analysis of the fractions. BN–PAGE is a technique that separates native protein complexes by size and charge, the latter provided by the anionic dye, Coomassie blue, which displaces the detergent used for solubilization. Although Scrib and Lgl2 co-sedimented in the gradients, surprisingly, only small amounts were found to co-IP and co-migrate in BN–PAGE. Two possibilities could explain this finding. Either the Scrib/Lgl2 association is weak and falls apart during BN–PAGE and co-IP or Lgl2 is in another complex whose size is comparable to the Scrib/Lgl2 complex. We favor the first and speculate that the Scrib/Lgl2 association may be transient with Lgl2 having a regulatory role.

In addition to the proteins identified in this study there are at least four other cytoplasmic proteins that have been reported to bind the PDZ domains of Scrib and could be in one or more of the Scrib complexes (Fig. 8). The first is high-risk human papilloma-virus E6 protein, which mediates the ubiquitination and subsequent degradation of both Scrib and Dlg [Nakagawa and Huibregtse, 2000]. Upon analysis of cervical [Nakagawa et al., 2004] and mammary tissue [Navarro et al., 2005], Scrib protein levels were decreased in neoplastic tissue relative to normal tissue supporting the hypothesis that Scrib is a tumor suppressor (for a review see [Bilder, 2004]). The second cytoplasmic protein is GUK Holder (GUKH), which was shown to bind the guanylate kinase (GUK) domain of Dlg and PDZ 2 domain of Scrib by co-IP and yeast two-hybrid analysis [Mathew et al., 2002]. In flies with reduced GUKH protein levels, Scrib but not Dlg mislocalizes to the cytosol of developing synapses. The third Scrib-binding partner, β-PIX, is a guanine nucleotide exchange factor (GEF), which requires Scrib to anchor it at the PM [Audebert et al., 2004]. Both proteins are involved in regulated exocytosis in PC12 cells [Audebert et al., 2004]. This complex is also found in a human mammary epithelial cell line indicating that Scrib's role in regulated exocytosis may be conserved in other cell types. The fourth Scrib-binding partner, ZO-2, localizes to the TJ [Gumbiner et al., 1991] and is regulated during cancer progression [Chlenski et al., 1999; Chlenski et al., 2000]. This association is mediated between Scrib's PDZ domains 3 and 4 and the C-terminal PDZ binding motif of ZO-2 [Metais et al., 2005]. Interestingly, Lgl2 is the only protein identified to date that associates with Scrib's LRR domain and not its PDZ domain.

### Scrib, Vangl2, and Epithelial Cell Polarity

Studies of Drosophila mutants exhibiting abnormal epithelial cell shape and organization led to the identification of evolutionarily conserved proteins required for the development of apical/basal polarity [Ohno, 2001; Bilder, 2003; Roh and Margolis, 2003]. Crumbs, Bazooka, and Scrib, the most prominent polarity complexes, are each composed of several multi-domain proteins. Recent reports of genetic interactions among different members of these complexes, together with careful phenotypic analyses of mutants, have led to models in which the three complexes coordinately regulate the development of apical/basal polarity [Bilder et al., 2003; Tanentzapf and Tepass, 2003].

All three complexes function at the PM. The membrane anchors for the Crumbs and Bazooka protein complexes in mammals have been identified as Crumbs and junction adhesion molecule (JAM), respectively. Both are single transmembrane proteins with C-terminal PDZ binding motifs [Hong et al., 2001; Itoh et al., 2001; Medina et al., 2002; Makarova et al., 2003]. Our morphological and biochemical studies are the first to show that Vangl2 is at the basolateral PM in polarized mammalian epithelial cells and is a membrane anchor for the Scrib complex. Vangl2 also has a C-terminal PDZ binding motif that, although not required for it's proper PM localization, is essential for binding to Scrib. We propose that Vangl2 prefers binding of two PDZs in tandem. This finding is unusual but not unprecedented, since the membrane protein Syndecan requires the two PDZ domains in Syntenin to bind [Grootjans et al., 2000]. Furthermore, Syntenin also binds weakly to the cytoplasmic domains of Neurexin and B-class ephrins via its tandem PDZ domains, suggesting that weak PDZ domain interactions may be used in targeting

the PDZ protein to a pre-existing molecular assembly rather than driving the latter's formation [Grootjans et al., 2000]. In this light, might Scrib's PDZ domains 2 and 3 act similarly to target it to Vangl2 in the basolateral PM? Alternatively, since the LRR domain also has basolateral targeting information, which may be dominant [Zeitler et al., 2004], binding of Vangl2 to PDZ domains 2 and 3 might stabilize the membrane-bound Scrib in an extended conformation to allow additional proteins to bind to other regions in Scrib. For example, partners for the LAP motifs, acidic region, PDZs 1 and 4, and C-terminal 437 aa have yet to be identified. Recently, a multi-step mechanism for Scrib's role in establishing cortical polarity in fly neuroblasts has been described [Albertson et al., 2004].

In addition to endo Scrib, we found that endo Dlg bound the C-terminus of Vangl confirming a previous report [Torban et al., 2004]. While we have not performed assays with recombinant proteins, our detection of only exogenous Scrib on Coomassie Blue-stained gels after extracts from transfected HEK293A cells were incubated with Vangl2 beads, strongly suggests that Scrib can interact directly with Vangl2. If another protein mediated Scrib's association with the beads, it should have been present in near-stoichiometric amounts.

The interactions among Scrib, Dlg, and Vangl at the lateral PM are complex and not fully resolved. For example, loss of Dlg in flies leads to loss of Scrib at the PM [Mathew et al., 2002] but not the reverse [Roche et al., 2002]. Likewise, loss of Vangl in flies leads to loss of Dlg at the PM [Mathew et al., 2002]. Unfortunately, Scrib was not examined. Nonetheless, the picture emerging has Vangl recruiting Dlg, which in turn recruits Scrib to bind Vangl2. Additional components, not yet identified, are likely to be involved.

### Final Comments

The results of the present study have clearly established that Lgl2 and Vangl2 associate with Scrib. There are undoubtedly additional molecules that interact with the multi-domain scaffold protein to form macromolecular complexes involved in many cellular processes whose underlying similarity is in their asymmetric nature. The challenge will be to first enumerate the compositions of the complexes and then define their roles spatially and temporally in different cellular backgrounds.

## ACKNOWLEDGMENTS

We thank YaHui Chen, Lydia Nyasae, Rebeca Yutzy, and Alfred See for technical assistance, Dr. Robert Jensen, Dr. Cory Dunn, and Matthew Youngman for advice and guidance regarding BN–PAGE and Dr. Debra Andrew and Dr. Douglas Robinson for critical reading of the manuscript. This work was supported by grants from the National Institutes of Health (GM064645 and DK63096 to A.L.H., DK07632 and DK64388 to M. Donowitz) and Johns Hopkins University School of Medicine.

## REFERENCES

Albertson R, Chabu C, Sheehan A, Doe CQ. 2004. Scribble protein domain mapping reveals a multistep localization mechanism and domains necessary for establishing cortical polarity. J Cell Sci 117:6061–6070. (Epub).

Araki N, Lee T, Matsubara H, Takashima Y. 1993. An improved technique for observing both membranous organelles and cytoskeleton in saponin-extracted cells. J Electron Microsc (Tokyo) 42:51–54.

Audebert S, Navarro C, Nourry C, Chasserot-Golaz S, Lecine P, Bellaiche Y, Dupont JL, Premont RT, Sempere C, Strub JM, Van Dorsselaer A, Vitale N, Borg JP. 2004. Mammalian scribble forms a tight complex with the betaPIX exchange factor. Curr Biol 14:987–995.

Ausubel FM, Brent R, Kingston RE, Moore DD, Seidman JD, Smith JA, Struhl K, Albright LM, Coen DM, Varki A, editors. 1995. Preparation and analysis of RNA. In: Current Protocols in Molecular Biology. Hoboken: John Wiley & Sons, Inc.

Barr VA, Hubbard AL. 1993. Newly synthesized hepatocyte plasma membrane proteins are transported in transcytotic vesicles in the bile duct-ligated rat. Gastroenterology 105:554–571.

Bilder D. 2003. PDZ domain polarity complexes. Curr Biol 13:R661–R662.

Bilder D. 2004. Epithelial polarity and proliferation control: Links from the Drosophila neoplastic tumor suppressors. Genes Dev 18:1909–1925.

Bilder D, Perrimon N. 2000. Localization of apical epithelial determinants by the basolateral PDZ protein Scribble. Nature 403:676–680.

Bilder D, Li M, Perrimon N. 2000. Cooperative regulation of cell polarity and growth by Drosophila tumor suppressors. Science 289:113–116.

Bilder D, Schober M, Perrimon N. 2003. Integrated activity of PDZ protein complexes regulates epithelial polarity. Nat Cell Biol 5:53–58.

Bryant PJ, Huwe A. 2000. LAP proteins: What's up with epithelia? Nat Cell Biol 2:E141–E143.

Chlenski A, Ketels KV, Tsao MS, Talamonti MS, Anderson MR, Oyasu R, Scarpelli DG. 1999. Tight junction protein ZO-2 is differentially expressed in normal pancreatic

ducts compared to human pancreatic adenocarcinoma. Int J Cancer 82:137–144.
Chlenski A, Ketels KV, Korovaitseva GI, Talamonti MS, Oyasu R, Scarpelli DG. 2000. Organization and expression of the human zo-2 gene (tjp-2) in normal and neoplastic tissues. Biochim Biophys Acta 1493:319–324.
Dow LE, Brumby AM, Muratore R, Coombe ML, Sedelies KA, Trapani JA, Russell SM, Richardson HE, Humbert PO. 2003. hScrib is a functional homologue of the Drosophila tumour suppressor Scribble. Oncogene 22:9225–9230.
Enkhbayar P, Kamiya M, Osaki M, Matsumoto T, Matsushima N. 2004. Structural principles of leucine-rich repeat (LRR) proteins. Proteins 54:394–403.
Greger IH, Khatri L, Kong X, Ziff EB. 2003. AMPA receptor tetramerization is mediated by Q/R editing. Neuron 40: 763–774.
Grootjans JJ, Reekmans G, Ceulemans H, David G. 2000. Syntenin-syndecan binding requires syndecan-synteny and the co-operation of both PDZ domains of syntenin. J Biol Chem 275:19933–19941.
Gumbiner B, Lowenkopf T, Apatira D. 1991. Identification of a 160-kDa polypeptide that binds to the tight junction protein ZO-1. Proc Natl Acad Sci USA 88:3460–3464.
Hardy S. 1997. Construction of adenovirus vectors through Cre-lox recombination. J Virol 71:1842–1849.
Harris B, Lim W. 2001. Mechanism and role of PDZ domains in signaling complex assembly. J Cell Sci 114: 3219–3231.
He TC, Zhou S, da Costa LT, Yu J, Kinzler KW, Vogelstein B. 1998. A simplified system for generating recombinant adenoviruses. Proc Natl Acad Sci USA 95:2509–2514.
Hong Y, Sstronach B, Perrimon N, Jan L, Jan Y. 2001. Drosophila Stardust interacts with Crumbs to control polarity of epithelia but not neuroblasts. Nature 414: 634–638.
Hubbard AL, Barr VA, Scott LJ. 1994. Hepatocyte surface polarity. In: Arias IM, Boyer JL, Fausto N, Jakoby WB, Schachter DA, Shafritz DA, editors. The liver: Biology and pathobiology, 3rd edition. New York: Raven Press, pp 189–213.
Hung AY, Sheng M. 2002. PDZ domains: Structural modules for protein complex assembly. J Biol Chem 277:5699–5702.
Ihrke G, Neufeld EB, Meads T, Shanks MR, Cassio D, Laurent M, Schroer TA, Pagano RE, Hubbard AL. 1993. WIF-B cells: An in vitro model for studies of hepatocyte polarity. J Cell Biol 123:1761–1775.
Itoh M, Sasaki H, Furuse M, Ozaki H, Kita T, Tsukita S. 2001. Junctional adhesion molecule (JAM) binds to PAR-3: A possible mechanism for the recruitment of PAR-3 to tight junctions. J Cell Biol 154:491–497.
Jessen JR, Solnica-Krezel L. 2004. Identification and developmental expression pattern of van gogh-like 1, a second zebrafish strabismus homologue. Gene Expr Patterns 4:339–344.
Jessen JR, Topczewski J, Bingham S, Sepich DS, Marlow F, Chandrasekhar A, Solnica-Krezel L. 2002. Zebrafish trilobite identifies new roles for Strabismus in gastrulation and neuronal movements. Nat Cell Biol 4:610–615.
Kajava AV, Kobe B. 2002. Assessment of the ability to model proteins with leucine-rich repeats in light of the latest structural information. Protein Sci 11:1082–1090.
Katoh M, Katoh M. 2004. Identification and characterization of human LLGL4 gene and mouse Llgl4 gene in silico. Int J Oncol 24:737–742.
Kobe B, Deisenhofer J. 1993. Crystal structure of porcine ribonuclease inhibitor, a protein with leucine-rich repeats. Nature 366:751–756.
Kobe B, Deisenhofer J. 1995. A structural basis of the interactions between leucine-rich repeats and protein ligands. Nature 374:183–186.
Kobe B, Deisenhofer J. 1996. Mechanism of ribonuclease inhibition by ribonuclease inhibitor protein based on the crystal structure of its complex with ribonuclease A. J Mol Biol 264:1028–1043.
Kobe B, Kajava AV. 2001. The leucine-rich repeat as a protein recognition motif. Curr Opin Struct Biol 11:725–732.
Koivisto UM, Hubbard AL, Mellman I. 2001. A novel cellular phenotype for familial hypercholesterolemia due to a defect in polarized targeting of LDL receptor. Cell 105:575–585.
Lee MC, Hamamoto S, Schekman R. 2002. Ceramide biosynthesis is required for the formation of the oligomeric H+-ATPase Pma1p in the yeast endoplasmic reticulum. J Biol Chem 277:22395–22401.
Lee OK, Frese KK, James JS, Chadda D, Chen ZH, Javier RT, Cho KO. 2003. Discs-Large and Strabismus are functionally linked to plasma membrane formation. Nat Cell Biol 5:987–993. (Epub 2003 Oct 19).
Legouis R, Jaulin-Bastard F, Schott S, Navarro C, Borg JP, Labouesse M. 2003. Basolateral targeting by leucine-rich repeat domains in epithelial cells. EMBO Rep 4:1096–1102. (Epub 2003 Oct 24).
Lehman K, Rossi G, Adamo JE, Brennwald P. 1999. Yeast homologues of tomosyn and lethal giant larvae function in exocytosis and are associated with the plasma membrane SNARE, Sec9. J Cell Biol 146:125–140.
Makarova O, Roh MH, Liu CJ, Laurinec S, Margolis B. 2003. Mammalian crumbs3 is a small transmembrane protein linked to protein associated with Lin-7 (Pals1). Gene 302:21–29.
Mathew D, Gramates LS, Packard M, Thomas U, Bilder D, Perrimon N, Gorczyca M, Budnik V. 2002. Recruitment of scribble to the synaptic scaffolding complex requires GUK-holder, a novel DLG binding protein. Curr Biol 12: 531–539.
Medina E, Lemmers C, Lane-Guermonprez L, Le Bivic A. 2002. Role of the Crumbs complex in the regulation of junction formation in Drosophila and mammalian epithelial cells. Biol Cell 94:305–313.
Metais JY, Navarro C, Santoni MJ, Audebert S, Borg JP. 2005. hScrib interacts with ZO-2 at the cell-cell junctions of epithelial cells. FEBS Lett 579:3725–3730.
Mevel-Ninio M, Weiss MC. 1981. Immunofluorescence analysis of the time-course of extinction, reexpression, and activation of albumin production in rat hepatoma-mouse fibroblast heterokaryons and hybrids. J Cell Biol 90:339–350.
Montcouquiol M, Rachel RA, Lanford PJ, Copeland NG, Jenkins NA, Kelley MW. 2003. Identification of Vangl2 and Scrb1 as planar polarity genes in mammals. Nature 423:173–177.
Murdoch JN, Rachel RA, Shah S, Beermann F, Stanier P, Mason CA, Copp AJ. 2001. Circletail, a new mouse

mutant with severe neural tube defects: Chromosomal localization and interaction with the loop-tail mutation. Genomics 78:55–63.

Murdoch JN, Henderson DJ, Doudney K, Gaston-Massuet C, Phillips HM, Paternotte C, Arkell R, Stanier P, Copp AJ. 2003. Disruption of scribble (Scrb1) causes severe neural tube defects in the circletail mouse. Hum Mol Genet 12:87–98.

Musch A, Cohen D, Yeaman C, Nelson WJ, Rodriguez-Boulan E, Brennwald PJ. 2002. Mammalian homolog of Drosophila tumor suppressor lethal (2) giant larvae interacts with basolateral exocytic machinery in Madin-Darby canine kidney cells. Mol Biol Cell 13: 158–168.

Nakagawa S, Huibregtse JM. 2000. Human scribble (Vartul) is targeted for ubiquitin-mediated degradation by the high-risk papillomavirus E6 proteins and the E6AP ubiquitin-protein ligase. Mol Cell Biol 20:8244–8253.

Nakagawa S, Yano T, Nakagawa K, Takizawa S, Suzuki Y, Yasugi T, Huibregtse JM, Taketani Y. 2004. Analysis of the expression and localisation of a LAP protein, human scribble, in the normal and neoplastic epithelium of uterine cervix. Br J Cancer 90:194–199.

Navarro C, Nola S, Audebert S, Santoni MJ, Arsanto JP, Ginestier C, Marchetto S, Jacquemier J, Isnardon D, Le Bivic A, Birnbaum D, Borg JP. 2005. Junctional recruitment of mammalian Scribble relies on E-cadherin engagement. Oncogene 24:4330–4339.

Ohno S. 2001. Intercellular junctions and cellular polarity: The PAR-aPKC complex, a conserved core cassette playing fundamental roles in cell polarity. Curr Opin Cell Biol 13:641–648.

Quillin ML, Matthews BW. 2000. Accurate calculation of the density of proteins. Acta Crystallogr D Biol Crystallogr 56(Pt 7):791–794.

Roche JP, Packard MC, Moeckel-Cole S, Budnik V. 2002. Regulation of synaptic plasticity and synaptic vesicle dynamics by the PDZ protein Scribble. J Neurosci 22: 6471–6479.

Roh MH, Margolis B. 2003. Composition and function of PDZ protein complexes during cell polarization. Am J Physiol Renal Physiol 285:F377–F387.

Santoni MJ, Pontarotti P, Birnbaum D, Borg JP. 2002. The LAP family: A phylogenetic point of view. Trends Genet 18:494–497.

Schagger H. 2001. Blue-native gels to isolate protein complexes from mitochondria. Methods Cell Biol 65: 231–244.

Segbert C, Johnson K, Theres C, van Furden D, Bossinger O. 2004. Molecular and functional analysis of apical junction formation in the gut epithelium of Caenorhabditis elegans. Dev Biol 266:17–26.

Sepich DS, Myers DC, Short R, Topczewski J, Marlow F, Solnica-Krezel L. 2000. Role of the zebrafish trilobite locus in gastrulation movements of convergence and extension. Genesis 27:159–173.

Shanks MR, Cassio D, Lecoq O, Hubbard AL. 1994. An improved polarized rat hepatoma hybrid cell line. Generation and comparison with its hepatoma relatives and hepatocytes in vivo. J Cell Sci 107:813–825.

Tanentzapf G, Tepass U. 2003. Interactions between the crumbs, lethal giant larvae and bazooka pathways in epithelial polarization. Nat Cell Biol 5:46–52.

Tomita S, Adesnik H, Sekiguchi M, Zhang W, Wada K, Howe JR, Nicoll RA, Bredt DS. 2005. Stargazin modulates AMPA receptor gating and trafficking by distinct domains. Nature 435:1052–1058.

Torban E, Wang HJ, Groulx N, Gros P. 2004. Independent mutations in mouse Vangl2 that cause neural tube defects in looptail mice impair interaction with members of the Dishevelled family. J Biol Chem 279:52703–52713. (Epub).

Yamanaka T, Horikoshi Y, Sugiyama Y, Ishiyama C, Suzuki A, Hirose T, Iwamatsu A, Shinohara A, Ohno S. 2003. Mammalian Lgl forms a protein complex with PAR-6 and aPKC independently of PAR-3 to regulate epithelial cell polarity. Curr Biol 13:734–743.

Yang T, Espenshade PJ, Wright ME, Yabe D, Gong Y, Aebersold R, Goldstein JL, Brown MS. 2002. Crucial step in cholesterol homeostasis: Sterols promote binding of SCAP to INSIG-1, a membrane protein that facilitates retention of SREBPs in ER. Cell 110:489–500.

Zeitler J, Hsu CP, Dionne H, Bilder D. 2004. Domains controlling cell polarity and proliferation in the Drosophila tumor suppressor Scribble. J Cell Biol 167:1137–1146.